Adaptive Beam Tracking with the Unscented Kalman Filter for Millimeter Wave Communication

Stephen G. Larew and David J. Love, *Fellow, IEEE*

***Abstract*—Millimeter wave (mmWave) communication links for 5G cellular technology require high beamforming gain to overcome channel impairments and achieve high throughput. While much work has focused on estimating mmWave channels and designing beamforming schemes, the time dynamic nature of mmWave channels quickly renders estimates stale and increases sounding overhead. We model the underlying time dynamic state space of mmWave channels with a linear Gauss-Markov process and design sounding beamformers suitable for tracking in an unscented Kalman filtering framework. Given an initial channel estimate, simulation results show that unscented filtering efficiently leads to better estimates than the extended Kalman filter with limited sounding and allows forward prediction for higher sustained beamforming gain during data transmission. Moreover, from tracked prior channel estimates, optimal and constrained suboptimal beams are adaptively chosen for low sounding overhead while minimizing estimation error.**

***Index Terms*—millimeter wave, beamforming, channel estimation, unscented Kalman filter, tracking.**

I. Introduction

MILLIMETER wavelength communication systems stand as an important pillar for Fifth Generation (5G) cellular standards [1]. Beyond the 6 GHz ceiling of current systems, the 20 to 100 GHz range of millimeter wave (mmWave) frequencies offers ample bandwidth for high throughputs but suffers from less favorable propagation conditions. High antenna count arrays at the transmitter and receiver can provide large beamforming gains to overcome the greater path loss and shadowing. The mmWave channel estimation and beamforming problem has been studied extensively [2]–[9]; [10]–[16] studied tracking and [17]–[25] specifically examined temporal channel state correlation models.

Suppose the mmWave multiple-input multiple-output (MIMO) channel that is to be estimated is parameterized by a set of state variables that evolve over time. If the transmitter and receiver know the state variables, then due to the parameterization of the channel model, they have full channel state information (CSI). With probabilistic information about a state space model of the channel, then statistical CSI is available. If the state variables stochastically evolve over time according to such a known model, the channel can be predicted into the future. Moreover, optimal sounding beams can be chosen given the channel predictions. Therefore, this work assumes the mmWave MIMO channel can be parameterized by a state space model and focuses on adaptively tracking channel state parameters over time.

Previous works [17]–[25] identified the path gains and angles of arrival and departure as candidate parameters for a state space model of the mmWave channel. While only the angles are modeled in [17], [19], and [20] adds path gains, both follow a simple zeroth-order motion model (i.e., innovations are entirely due to a noise process). A first-order model with linear motion for angles is described in [22] but the model is nonlinear and specific to the discrete lens array; [24] similarly constrains the physical geometry and beam architecture. In this work, the proposed time evolution model for the state space parameters is linear in Cartesian space, not tied to a specific mmWave array architecture, and extends to higher-order motion models.

Although the state evolution model of this work is linear, the channel observation model is generally nonlinear. For tracking channel state, the extended Kalman filter (EKF) is based on a linear approximation around the current state of the nonlinear model. The conditions and assumptions allowing the linearization to proceed with minimal error are dependent on the current state estimate, the covariance magnitude, and the transformation, which may be time-varying [26]. Moreover, the Jacobian matrices are non-constant and generally must be derived, either analytically or computationally, as a function of the sounding beams. Thus, as the system diverges from the original design conditions or the linearization weakens, the EKF offers uncertain performance with high computational overhead.

The unscented Kalman filter (UKF) [27] offers an alternative suboptimal approximation given the intractability of recursive Bayesian estimation and the weaknesses of the EKF. The UKF adapts the standard Kalman filter framework, which is the optimal solution for linear Gaussian systems, with an alternative to the linearization of the EKF. Key to the UKF, the unscented transform propagates means and covariances through nonlinearities with improved accuracy. This work employs the UKF because it 1) readily adapts to model changes, 2) presents a black box approach that scales with the state dimensions with similar complexity to the first-order EKF, 3) generalizes to any mmWave hardware architecture, and 4) trivially supports adaptive sounding because it is not dependent on a Jacobian matrix that may be a function of the adaptively chosen sounding beams.

This work presents a linear extensible motion model, demonstrates the UKF as an advantageous tracking technique over the EKF, and shows the form of optimal and suboptimal sounding beams to adaptively track the mmWave channel.

In addition to standard notations, $\mathbf{A}_{[b:c]}$ is the matrix

Stephen G. Larew was supported in part by the National Science Foundation (NSF) Graduate Research Fellowship Program under Grant No. DGE-1333468; David J. Love was supported by the NSF under grant CNS1642982. The authors are with the School of Electrical and Computer Engineering, Purdue University, West Lafayette, IN 47907 USA e-mail: sglarew@alumni.purdue.edu.

from the b-th to the c-th columns of $\mathbf{A}$; tilde converts from complex to real vector spaces: $\tilde{\mathbf{a}} = [\mathrm{Re}(\mathbf{a}^{\mathsf{T}})\,\mathrm{Im}(\mathbf{a}^{\mathsf{T}})]^{\mathsf{T}}$ and $\tilde{\mathbf{A}} = [\mathrm{Re}(\mathbf{A}) - \mathrm{Im}(\mathbf{A}); \mathrm{Im}(\mathbf{A})\ \mathrm{Re}(\mathbf{A})]$; second-order circular random vector $\mathbf{a} = \mathbf{x} + j\mathbf{y}$ has real covariance $\mathbb{E}\left\{\tilde{\mathbf{a}}\tilde{\mathbf{a}}^T\right\} = [\mathbb{E}\left\{\mathbf{x}\mathbf{x}^{\mathsf{T}}\right\}\ \mathbb{E}\left\{\mathbf{x}\mathbf{y}^{\mathsf{T}}\right\}; \mathbb{E}\left\{\mathbf{y}\mathbf{x}^{\mathsf{T}}\right\}\ \mathbb{E}\left\{\mathbf{y}\mathbf{y}^{\mathsf{T}}\right\}]$; $\mathbf{I}_N$ is the $N \times N$ identity; $\mathrm{vec}(\mathbf{A})$ stacks columns of $\mathbf{A}$ into a vector.

II. System Model and Problem Formulation

A. Millimeter Wave Communication Model

Consider transmission and reception with M_{T} and M_{R} antennas, respectively. For each coherence period k, the transmitter scales a symbol $s_k \in \mathbb{C}$ with the beamformer $\mathbf{f}_k \in \mathbb{C}^{M_{\mathrm{T}}}$ before transmission over the MIMO channel $\mathbf{H}_k$. At the receiver, the combiner $\mathbf{z}_k \in \mathbb{C}^{M_{\mathrm{R}}}$ scales the noisy received signal before the channel outputs are summed to form the received sample r_k. From input to output, the ith beamformed and combined noisy channel output during the kth channel coherence period is

$$r_k[i] = \mathbf{z}_k^H[i]\big(\mathbf{H}_k\mathbf{f}_k[i]s_k[i] + \mathbf{n}_k[i]\big). \tag{1}$$

The noise $\mathbf{n}_k[i] \sim \mathcal{CN}(\mathbf{0}, \frac{1}{\rho}\mathbf{I}_{M_{\mathrm{R}}})$ is independent and identically distributed across space and time. The beams, a nonspecific term referring to either a transmit beamformer or receive combiner, are unit-norm constrained, i.e., $\|\mathbf{f}_k\|_2 = \|\mathbf{z}_k\|_2 = 1$.

To estimate CSI, the transmitter and receiver sound beams during a channel coherence period.[1] For each of the N_{T} transmit sounding beams in the columns of $\mathbf{F}_k \in \mathbb{C}^{M_{\mathrm{T}} \times N_{\mathrm{T}}}$, the receiver sounds the beams in the columns of $\mathbf{Z}_k \in \mathbb{C}^{M_{\mathrm{R}} \times N_{\mathrm{R}}}$. During the kth coherence period, the $i = 1, \ldots, N_{\mathrm{R}}N_{\mathrm{T}}$ channel observations $r_k[i]$ form a noisy version of the matrix $\mathbf{Z}_k^H\mathbf{H}_k\mathbf{F}_k$.

B. Millimeter Wave Channel Model for Tracking

We extract the parameters for a common mmWave channel model [5] into a time dynamic state space model. The channel is modeled with array steering vectors for the arriving and departing plane waves. Consider the one-dimensional uniform linear array (ULA)[2] of M antennas with antenna separation d, for which the array steering vector is

$$\mathbf{a}(\phi) = \begin{bmatrix} e^{-j2\pi\phi} & \cdots & e^{-j2\pi m\phi} & \cdots & e^{-j2\pi M\phi} \end{bmatrix}^{\mathsf{T}}. \tag{2}$$

The angle of arrival $\theta \in [0, 2\pi)$ relates to the normalized spatial angle $\phi = \frac{d}{\lambda}\sin\theta$, where λ is the wavelength. The ℓth of L paired angle of departures (AOD) and angle of arrivals (AOA) from the transmitter to the receiver has gain $\alpha_\ell \sim \mathcal{CN}(0, 1)$ and normalized spatial AOA $\phi_{\mathrm{R},\ell}$ and AOD $\phi_{\mathrm{T},\ell}$. The narrowband slowly varying MIMO channel at time k is

$$\mathbf{H}_k = \sum_{\ell=1}^{L} \alpha_{k,\ell}\mathbf{a}\left(\phi_{\mathrm{R},k,\ell}\right)\mathbf{a}^H\left(\phi_{\mathrm{T},k,\ell}\right), \tag{3}$$

where the channel parameters $\alpha_{k,\ell}$, $\phi_{\mathrm{R},k,\ell}$, and $\phi_{\mathrm{T},k,\ell}$ for $\ell = 1, \ldots, L$ fully describe a given channel instance at time k.

[1] Intuitively, we can assume $s_k[i] = 1$ without loss of generality because the actual system will use a suitable sounding sequence.

[2] Other geometries, such as the uniform planar array, should not change the broad methods of this paper.

Each multipath between the transmitter and receiver is modeled by a position and velocity in Cartesian space[3], which together form the state. A position[4] ν is related to its AOD or AOA θ by $\nu = \tan(\theta)$. Thus, the normalized spatial angle ϕ relates to ν with

$$\phi = \frac{d}{\lambda}\sin\left(\arctan\left(\nu\right)\right). \tag{4}$$

As a first-order approximation to the dynamics of the multipaths, also consider the first time derivative (velocity) $\dot{\nu}_{a,\ell} = \frac{\mathrm{d}}{\mathrm{d}t}\nu_{a,\ell}$ of the positions.

For a single channel realization $\mathbf{H}$ (temporarily dropping the time subscript), the state space includes the positions $\nu_{a,\ell}$, velocities $\dot{\nu}_{a,\ell}$, and gains α_ℓ of the $\ell = 1, \ldots, L$ multipaths in relation to the transmitter ($a = \mathrm{T}$) and receiver ($a = \mathrm{R}$). The complete state space that parameterizes the channel is

$$\mathbf{x} = \mathrm{vec}\begin{bmatrix}\mathbf{x}^{(\alpha)} & \mathbf{x}^{(\nu_{\mathrm{T}})} & \mathbf{x}^{(\nu_{\mathrm{R}})}\end{bmatrix}, \tag{5}$$

$$\mathbf{x}^{(\alpha)} = \begin{bmatrix}\mathrm{Re}\,\alpha_1 & \mathrm{Im}\,\alpha_1 & \cdots & \mathrm{Re}\,\alpha_L & \mathrm{Im}\,\alpha_L\end{bmatrix}^{\mathsf{T}}, \tag{6}$$

$$\mathbf{x}^{(\nu_a)} = \begin{bmatrix}\nu_{a,1} & \dot{\nu}_{a,1} & \cdots & \nu_{a,L} & \dot{\nu}_{a,L}\end{bmatrix}^{\mathsf{T}}. \tag{7}$$

The relative motion of the transmitter and receiver and changes in the environment between the two result in both macro level motion, modeled with a velocity $\dot{\nu}$ on position ν, and micro level motion, modeled as an additive random process. Path gains are temporally correlated through a first-order Gauss-Markov process. The overall discrete-time dynamic model for time step T_{S} is

$$\mathbf{x}_k = \mathbf{A}_k\mathbf{x}_{k-1} + \mathbf{u}_k, \tag{8}$$

$$\mathbf{A}_k = \mathrm{blockdiag}\left(\beta_k\mathbf{I}_{2L}, \mathbf{I}_{2L} \otimes \begin{bmatrix}1 & T_{\mathrm{S}}\\ 0 & 1\end{bmatrix}\right), \tag{9}$$

where the process noise vector $\mathbf{u}_k \sim \mathcal{N}(\mathbf{0}, \mathbf{Q}_k)$. With each path gain independent of others and following a first order Gauss-Markov property, the upper $2L$ diagonal noise variances of $\mathbf{Q}_k$ are $(1 - \beta_k^2)/2$. The process noise for position and derivative pairs is white Gaussian noise.

C. Real Channel Observation Model

For the channel tracking problem, the observation model (1) is transformed from a complex to a real number representation to match the real number space used in the state evolution model. Vectorizing the sounding outputs with a property of the Kronecker product [28] gives

$$\mathrm{vec}\left[\mathbf{Z}_k^H\mathbf{H}\left(\mathbf{x}_k\right)\mathbf{F}_k\right] = \left(\mathbf{F}_k^{\mathsf{T}} \otimes \mathbf{Z}_k^H\right)\mathrm{vec}\left[\mathbf{H}\left(\mathbf{x}_k\right)\right], \tag{10}$$

where $\mathbf{H}(\mathbf{x}_k)$ is (3) evaluated with the state in $\mathbf{x}_k$. Defining the observation matrix $\mathbf{G}_k = \mathbf{F}_k^{\mathsf{T}} \otimes \mathbf{Z}_k^H$ and the vector channel $\mathbf{h}(\mathbf{x}_k) = \mathrm{vec}\,\mathbf{H}(\mathbf{x}_k)$, the noisy channel observation for the kth state is $\mathbf{y}_k = \mathbf{G}_k\mathbf{h}(\mathbf{x}_k) + \mathbf{v}_k$, The real-valued channel observation model is

$$\tilde{\mathbf{y}}_k = \tilde{\mathbf{G}}_k\tilde{\mathbf{h}}(\mathbf{x}_k) + \tilde{\mathbf{v}}_k, \tag{11}$$

where $\tilde{\mathbf{v}}_k \sim \mathcal{N}\left(\mathbf{0}, 1/2/\rho\mathbf{I}\right)$ is additive white Gaussian observation noise that is independent from the process noise.

[3] If motion is modeled in angular (θ) space, then even a first-order linear model would be nonlinear in Cartesian space (i.e., a simple constant speed multipath source is nonlinear in θ space).

[4] Without loss of generality, we project the position of a multipath onto a plane parallel to and of unit distance from the antenna array.

TABLE I
UKF PREDICTION AND UPDATE EQUATIONS

Prediction Variable	Equation
State Estimate	$\hat{\mathbf{x}}_{k\|k-1} = \mathbf{A}_k \hat{\mathbf{x}}_{k-1}$
State Covariance	$\mathbf{R}_{k\|k-1} = \mathbf{A}_k \mathbf{R}_{k-1} \mathbf{A}_k^{\mathsf{T}} + \mathbf{Q}_k$
Channel Estimate	$\hat{\mathbf{h}}_k = \sum_{i=0}^{12L} \omega_i^{(m)} \boldsymbol{\zeta}_i$
Channel Covariance	$\tilde{\mathbf{\Pi}}_k = \sum_{i=0}^{12L} \omega_i^{(c)} \left(\boldsymbol{\zeta}_i - \hat{\mathbf{h}}\right)\left(\boldsymbol{\zeta}_i - \hat{\mathbf{h}}\right)^{\mathsf{T}}$
Update Variable	**Equation**
Innovation	$\bar{\mathbf{y}}_k = \tilde{\mathbf{y}}_k - \tilde{\mathbf{G}}_k \hat{\mathbf{h}}_k$
Covariance	$\tilde{\mathbf{S}}_k = \tilde{\mathbf{G}}_k \tilde{\mathbf{\Pi}}_k \tilde{\mathbf{G}}_k^{\mathsf{T}} + 1/(2\rho)\mathbf{I}$
Cross-covariance	$\tilde{\mathbf{\Psi}}_k = \sum_{i=0}^{12L} \omega_i^{(c)} \left(\boldsymbol{\chi}_i - \hat{\mathbf{x}}_{k\|k-1}\right)\left(\boldsymbol{\zeta}_i - \hat{\mathbf{h}}_k\right)^{\mathsf{T}}$
State Estimate	$\hat{\mathbf{x}}_k = \hat{\mathbf{x}}_{k\|k-1} + \tilde{\mathbf{\Psi}}_k \tilde{\mathbf{G}}_k^{\mathsf{T}} \tilde{\mathbf{S}}_k^{-1} \bar{\mathbf{y}}_k$
State Covariance	$\mathbf{R}_k = \mathbf{R}_{k\|k-1} - \tilde{\mathbf{\Psi}}_k \tilde{\mathbf{G}}_k^{\mathsf{T}} \tilde{\mathbf{S}}_k^{-1} \tilde{\mathbf{G}}_k \tilde{\mathbf{\Psi}}_k^{\mathsf{T}}$

D. Problem Description

Design an observation matrix $\mathbf{G}_k = \mathbf{F}_k^{\mathsf{T}} \otimes \mathbf{Z}_k^H$ and track the current channel state $\mathbf{x}_k$ of the system from the observations $\mathbf{y}_{1:k} = \{\mathbf{y}_i : i = 1, \ldots, k\}$. The two problems are as follows.

1) Track the current channel state $\mathbf{x}_k$ from $\mathbf{y}_{1:k}$.
2) Design low overhead sounding beams.

III. Adaptive Channel Tracking

To improve the communication system performance and reduce estimation overhead, this section develops a tracking method for the channel parameters given an initial estimate. The channel model (3) is a nonlinear function of the state space (5) that evolves over time according to (8). Together, (8) and (11) form a discrete-time dynamic system.

Optimal Bayesian estimation of the current channel state $\mathbf{x}_k$ from the observations $\mathbf{y}_{1:k}$ involves recursively updating the posterior density $p(\mathbf{x}_k|\mathbf{y}_{1:k})$ to derive the minimum mean square estimator $\hat{\mathbf{x}}_k = \mathbb{E}\{\mathbf{x}_k|\mathbf{y}_{1:k}\}$. Finding the densities or the MMSE estimator is generally only tractable for linear Gaussian systems, in which case the Kalman filter is the exact optimal recursive solution. The nonlinear and non-Gaussian properties of our model require approximate solutions.

A. Suboptimal Estimation with UKF

In this work, the UKF is employed for state estimation and tracking. The UKF does not require computation of the Jacobian of $\frac{\partial \mathbf{G}_k \mathbf{h}(\mathbf{x})}{\partial \mathbf{X}}|_{\hat{\mathbf{x}}_{k|k-1}}$, which will be important when we consider adaptively designing $\mathbf{G}_k$ in Section III-B. Key to the UKF is the unscented transform, which estimates the posterior distribution of a transformed random variable by propagating mean and covariance of the prior through the nonlinear function by way of *sigma points* [27]. See [26], [27], [29] for full treatments of the UKF.

The UKF tracking equations in Table I begin with an unspecified channel estimator that gives the initial state estimate $\hat{\mathbf{x}}_0$ and its covariance $\mathbf{R}_0$. Recursively, given the previous state estimate $\hat{\mathbf{x}}_{k-1}$ and its covariance $\mathbf{R}_{k-1}$, the state in the kth block is predicted to be $\hat{\mathbf{x}}_{k|k-1}$ with covariance $\mathbf{R}_{k|k-1}$.

The statistics of channel $\tilde{\mathbf{h}}(\mathbf{x}_k)$ are approximated with the symmetric set of sigma points $\{\boldsymbol{\chi}_i\}_{i=0}^{12L}$ that approximate $\hat{\mathbf{x}}_{k|k-1}$ and $\mathbf{R}_{k|k-1}$. Let $\boldsymbol{\chi}_0 = \hat{\mathbf{x}}_{k|k-1}$ and let the weights be $\omega_0^{(m)} = \frac{\lambda}{6L+\lambda}, \omega_0^{(c)} = \frac{\lambda}{6L+\lambda} + (1 - \eta^2 + \mu), \omega_k^{(c)} = \omega_k^{(m)} = \frac{1}{2(6L+\lambda)}, k = 1, \ldots, 12L$ where $\lambda = \eta^2(6L + \kappa) - 6L$ ($\eta = 10^{-2}$, $\kappa = 0$, $\mu = 2$ are described in [30]). Sigma point design and parameter selection [31] affects filter performance as seen in Section IV. The remaining sigma points are $\boldsymbol{\chi}_i = \hat{\mathbf{x}}_{k|k-1} \pm \left(\sqrt{(6L+\lambda)\mathbf{R}_{k|k-1}}\right)_i$, where $(\sqrt{\mathbf{R}})_i$ denotes the ith column of the matrix square root of $\mathbf{R}$.

Transforming the sigma points through the channel gives $\{\boldsymbol{\zeta}_i = \tilde{\mathbf{h}}(\boldsymbol{\chi}_i)\}_{i=0}^{12L}$. The (approximate) predicted mean and covariance of the real channel[5] are, respectively, $\hat{\mathbf{h}}_k$ and $\tilde{\mathbf{\Pi}}_k$ (Table I). The Kalman filter update then gives the innovation $\bar{\mathbf{y}}_k$ and its (approximate) covariance $\tilde{\mathbf{S}}_k$. Finally, the updated state estimate $\hat{\mathbf{x}}_k$ has covariance

$$\mathbf{R}_k = \mathbf{R}_{k|k-1} - \tilde{\mathbf{\Psi}}_k \tilde{\mathbf{G}}_k^{\mathsf{T}} \tilde{\mathbf{S}}_k^{-1} \tilde{\mathbf{G}}_k \tilde{\mathbf{\Psi}}_k^{\mathsf{T}}. \tag{12}$$

Note that the UKF is entirely in the real number field (denoted by the tilde in Table I) to ensure the state update is not complex.

B. Adaptive Channel Sounding

This section provides an adaptive design technique for optimal and suboptimal sounding beams when tracking the channel. At each sounding, beams are chosen to optimize an objective function; between the mean squared error and average receive SNR metrics [32], minimizing the mean squared error $\mathrm{Tr}(\mathbf{R}_k)$ of the channel state is more general as it pursues overall accuracy of the channel estimate under the model.

The general design technique for adaptive channel sounding chooses beams for the k-th sounding that are optimizers of

$$\underset{\mathbf{F}_k \in \mathcal{F}, \mathbf{Z}_k \in \mathcal{Z}}{\arg\min} \quad \mathrm{Tr}\left(\tilde{\mathbf{W}} \mathbf{R}_k\right), \tag{13}$$

where $\tilde{\mathbf{W}}$ is a positive definite weighting matrix[6], and $\mathcal{F}$ and $\mathcal{Z}$ are feasible (constrained) sets of sounding beams.

An optimal but *infeasible* solution is first derived to guide the beam design problem. Substituting (12) into (13), converting from real to complex, and rearranging terms using the fact that matrix trace is invariant under cyclic permutations gives

$$\underset{\mathbf{F}_k \in \mathcal{F}, \mathbf{Z}_k \in \mathcal{Z}}{\arg\max} \quad \mathrm{Tr}\left(\mathbf{S}_k^{-1} \mathbf{G}_k \mathbf{\Psi}^H \mathbf{W} \mathbf{\Psi} \mathbf{G}_k^H\right). \tag{14}$$

Then, if $\mathbf{G}_k \mathbf{G}_k^H = \mathbf{I}$ then $\mathbf{S}_k = \mathbf{G}_k(\mathbf{\Pi}_k + 1/(\rho)\mathbf{I})\mathbf{G}_k^H$. The objective function then takes the form $\mathrm{Tr}((\mathbf{V}^H \mathbf{B} \mathbf{V})^{-1} \mathbf{V}^H \mathbf{A} \mathbf{V})$, which is the block generalized Rayleigh quotient (GRQ) with respect to the matrix pencil $(\mathbf{A}, \mathbf{B})$. Thus, by a property of the GRQ [33, p. 81-82], if $\mathbf{V}$ consists of the ordered normalized generalized eigenvectors[7] of $\mathbf{A} = \mathbf{\Psi}^H \mathbf{W} \mathbf{\Psi}$ and $\mathbf{B} = \mathbf{\Pi}_k + \frac{1}{\rho}\mathbf{I}$, then $\mathbf{G}_k^H = \mathbf{V}_{[1:N_{\mathrm{T}} N_{\mathrm{R}}]}$ is a global maximizer of (14) and thus a global minimizer of (13) when the sounding beams are unconstrained (i.e., $\mathcal{F} = \mathbb{C}^{M_{\mathrm{T}} \times N_{\mathrm{T}}}, \mathcal{Z} = \mathbb{C}^{M_{\mathrm{R}} \times N_{\mathrm{R}}}$) and the Kronecker product constraint in $\mathbf{G}_k$ is *ignored*.

Suboptimal, but *feasible*, sounding beams follow from the nearest constrained Kronecker product to $\mathbf{V}_{[1:N_{\mathrm{T}} N_{\mathrm{R}}]}$, which is

$$\underset{\mathbf{F} \in \mathcal{F}, \mathbf{Z} \in \mathcal{Z}}{\arg\min} \quad \left\|\mathbf{V}_{[1:N_{\mathrm{T}} N_{\mathrm{R}}]} - \mathbf{F}^* \otimes \mathbf{Z}\right\|_F. \tag{15}$$

[5]Second-order circularity of $\mathbf{h}(\mathbf{x}_k)$ implies zero pseudo-covariance.
[6]Among other uses, $\tilde{\mathbf{W}}$ allows favoring specific multipaths.
[7]i.e., $\mathbf{AV} - \mathbf{BV\Lambda} = \mathbf{0}, \mathbf{\Lambda} = \mathrm{diag}(\lambda_1, \lambda_2, \ldots), \lambda_1 \geq \lambda_2 \geq \cdots$

Optimizers for (15) when sounding beams are unconstrained follow from the best rank-one approximation of $\mathbf{U}$, which is a rearranged $\mathbf{V}_{[1:N_\mathrm{T}N_\mathrm{R}]}$ that matches the rearrangement of terms from $\mathbf{F}^* \otimes \mathbf{Z}$ to the outer product $\mathrm{vec}(\mathbf{F}^*)\,\mathrm{vec}(\mathbf{Z})^\mathsf{T}$ [34], giving

$$\underset{\mathbf{F}\in\mathcal{F},\mathbf{Z}\in\mathcal{Z}}{\arg\min} \quad \left\| \mathbf{U} - \mathrm{vec}\left(\mathbf{F}^*\right)\mathrm{vec}\left(\mathbf{Z}\right)^\mathsf{T} \right\|_F . \tag{16}$$

From the preceding development of optimal and suboptimal sounding beams, the following proposition is now proved.

Proposition 1: Optimizers $\mathbf{F}$ and $\mathbf{Z}$ of (16) minimize CSI covariance $\mathrm{Tr}\left(\mathbf{R}_k\right)$ if the objective function equals zero and the optimizing beams in $\mathbf{F}$ and $\mathbf{Z}$ are orthonormal or $\mathbf{G}_k\mathbf{G}_k^H = \mathbf{I}$.

Dominant left and right singular vectors of $\mathbf{U}$ minimize the objective of (16) but are unlikely to fall in the feasible sets $\mathcal{F}$ and $\mathcal{Z}$ for any realistic mmWave architecture. In fact, with $\mathbf{V}$ being unitary, it does not follow that orthonormal beams in $\mathbf{F}$ and $\mathbf{Z}$ will minimize (15) [34]. For realistic constraint sets on the sounding beams (e.g., equal gain, quantized phase, or DFT beam constraints [35]), the system designer could solve for approximations to the dominant singular vector solution to (16). A power method [36] for solving for the dominant singular vectors could be initialized with the previous time step's solution for potentially faster convergence. For the simulations we perform a unit normalization on the beams in the dominant singular vector solution to (16).

IV. Simulation Results

Results in this section demonstrate tracking of our channel model for select scenarios. Channel paths are independently and uniformly distributed across all AoD and AoA with the first derivative of the position $\dot{\nu}$ initially drawn from the Rayleigh distribution with scale $\sigma_{\dot{\nu}} = 100\sqrt{2/\pi}$ and multiplied by -1 with probability one-half. Other simulation parameters are initial position estimates $\hat{\nu} \sim \mathcal{N}(\nu, 0.1)$, initial velocities $\hat{\dot{\nu}} \sim \mathcal{N}(0, 10^6)$, and gain correlation $\beta = 0.905$. Process noise for positions and velocities is Gaussian with variance $10^{-6}/T_\mathrm{S}^2$ and $10^{-4}/T_\mathrm{S}^2$, respectively. Sounding beams for observations are chosen as described in Sec. III-B with normalization.

Fig. 1 shows a representative example of the time evolution of the AoD of 4 multipaths at $\rho = 5$ dB, $M_\mathrm{T} = M_\mathrm{R} = 16$, and after refinement $N_\mathrm{T} = N_\mathrm{R} = 6$. Fifty channel observations with suboptimal beams are taken every $T_\mathrm{S} = 0.1$ ms. Between observations, state updates and predictions are made every 1 μs. To start, the tracked estimates suffer from the error in the initial estimates and lack of position velocities. By 1 ms, the tracked AoDs stabilize on the correct positions and estimated velocities converge. From 2 to 5 ms, good tracking continues despite the crossing of paths.

Fig. 2 shows the mean squared error (MSE) of a path's angle of departure when sounding with a small number of the optimal and suboptimal beams of Section III-B. Both 8x8 and 16x16 arrays are simulated with $N_\mathrm{T} = N_\mathrm{R} = 2$ sounding beams every $T_\mathrm{S} = 10^{-4}$ s. We compare to the EKF [24] for reference. Monte Carlo simulation with 10 000 converging iterations produced samples to compute $\theta_{\mathrm{MSE},k} = \mathbb{E}\left\{|\hat{\theta}_k - \theta_k|^2\right\}$ and then averaging over $\theta_{\mathrm{MSE},k}$ for $k = 1, \ldots, 20$ produced the MSE for each ρ. With higher SNRs, the performance gap of

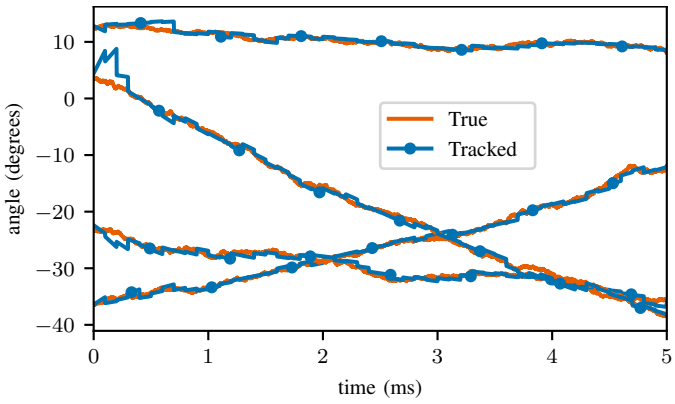

Fig. 1. Example of time evolution of four multipaths and their estimates.

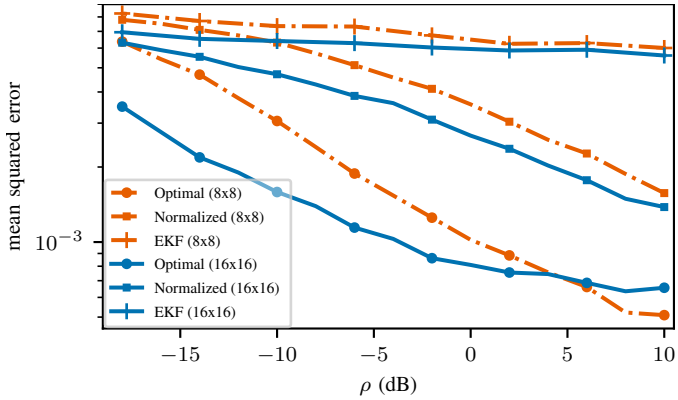

Fig. 2. Mean squared error of $\theta = \arctan(\nu)$ for the optimal combined beams $\mathbf{G}^H = \mathbf{V}_{[1:N_\mathrm{T}N_\mathrm{R}]}$ and the feasible normalized beams from solving (16) for $M_\mathrm{T} = M_\mathrm{R} = 8$ and $M_\mathrm{T} = M_\mathrm{R} = 16$.

the optimal beams increases over the suboptimal but feasible beams. However, the standard deviation of the error ranges from about 2 to 5 degrees for a single path[8]. The importance of the design and parameters defining the sigma points relative to the antenna count shows around $\rho = 5$ dB, where the optimal beams for the 8x8 array overtake the 16x16 array in MSE performance.

V. Conclusions

A time dynamic channel model was proposed and both a recursive channel tracking algorithm (based on the UKF) and an adaptive sounding beam selection process were presented. The channel model builds on static models by considering physical intuitions of the multipaths. Moreover, the channel model as presented can be extended (e.g., higher-order path motion) or modified considerably so long as a simple state space model can be derived. Channel tracking with optimal and constrained suboptimal beams enables prediction of CSI between soundings and reduces the sounding overhead. Simulation results show promising tracking performance. Future work may consider limited-feedback for CSI [32], [37], adaptive sigma point design, and more specific constrained beam sets reflecting hybrid analog and digital mmWave architectures.

[8]Estimation error should be interpreted relative to the AoD. Broadside AoDs need lower error due to the narrower half power beam width.

REFERENCES

[1] J. G. Andrews, S. Buzzi, W. Choi, S. V. Hanly, A. Lozano, A. C. K. Soong, and J. C. Zhang, "What will 5G be?" *IEEE J. Sel. Areas Commun.*, vol. 32, no. 6, pp. 1065–1082, June 2014.

[2] A. Alkhateeb, O. El Ayach, G. Leus, and R. W. Heath, "Channel estimation and hybrid precoding for millimeter wave cellular systems," *IEEE J. Sel. Topics Signal Process.*, vol. 8, no. 5, pp. 831–846, Oct 2014.

[3] S. Hur, T. Kim, D. J. Love, J. V. Krogmeier, T. A. Thomas, and A. Ghosh, "Millimeter wave beamforming for wireless backhaul and access in small cell networks," *IEEE Trans. Commun.*, vol. 61, no. 10, pp. 4391–4403, October 2013.

[4] A. Alkhateeb, J. Mo, N. Gonzalez-Prelcic, and R. Heath, "MIMO precoding and combining solutions for millimeter-wave systems," *IEEE Commun. Mag.*, vol. 52, no. 12, pp. 122–131, December 2014.

[5] R. W. Heath, N. González-Prelcic, S. Rangan, W. Roh, and A. M. Sayeed, "An overview of signal processing techniques for millimeter wave MIMO systems," *IEEE J. Sel. Topics Signal Process.*, vol. 10, no. 3, pp. 436–453, April 2016.

[6] M. Xiao, S. Mumtaz, Y. Huang, L. Dai, Y. Li, M. Matthaiou, G. K. Karagiannidis, E. Björnson, K. Yang, C. L. I, and A. Ghosh, "Millimeter wave communications for future mobile networks," *IEEE J. Sel. Areas Commun.*, vol. 35, no. 9, pp. 1909–1935, Sept 2017.

[7] S. Kutty and D. Sen, "Beamforming for millimeter wave communications: An inclusive survey," *IEEE Commun. Surveys Tuts.*, vol. PP, no. 99, pp. 1–1, 2015.

[8] O. El Ayach, S. Rajagopal, S. Abu-Surra, Z. Pi, and R. Heath, "Spatially sparse precoding in millimeter wave MIMO systems," *IEEE Trans. Wireless Commun.*, vol. 13, no. 3, pp. 1499–1513, March 2014.

[9] J. Song, J. Choi, S. G. Larew, D. J. Love, T. A. Thomas, and A. A. Ghosh, "Adaptive millimeter wave beam alignment for dual-polarized MIMO systems," *IEEE Trans. Wireless Commun.*, vol. 14, no. 11, pp. 6283–6296, Nov 2015.

[10] D. Zhang, H. Chen, M. Shirvanimoghaddam, Y. Li, and B. Vucetic, "Training beam sequence optimization for millimeter wave MIMO tracking systems," in *2018 IEEE International Conference on Communications (ICC)*, May 2018, pp. 1–6.

[11] D. Zhu, J. Choi, Q. Cheng, W. Xiao, and R. W. Heath, "High-resolution angle tracking for mobile wideband millimeter-wave systems with antenna array calibration," *IEEE Trans. Wireless Commun.*, vol. 17, no. 11, pp. 7173–7189, Nov 2018.

[12] H. S. Ghadikolaei, H. Ghauch, and C. Fischione, "Learning-based tracking of AoAs and AoDs in mmWave networks," in *Proceedings of the 2Nd ACM Workshop on Millimeter Wave Networks and Sensing Systems*, ser. mmNets '18. New York, NY, USA: ACM, 2018, pp. 45–50. [Online]. Available: http://doi.acm.org/10.1145/3264492.3264500

[13] K. Upadhya, S. A. Vorobyov, and R. W. Heath, "Low-overhead receiver-side channel tracking for mmWave MIMO," in *2018 IEEE International Conference on Acoustics, Speech and Signal Processing (ICASSP)*, April 2018, pp. 3859–3863.

[14] J. Seo, Y. Sung, G. Lee, and D. Kim, "Training beam sequence design for millimeter-wave MIMO systems: A POMDP framework," *IEEE Trans. Signal Process.*, vol. 64, no. 5, pp. 1228–1242, March 2016.

[15] D. Zhang, H. Chen, M. Kokshoorn, Y. Li, N. Wei, and B. Vucetic, "A probe-then-refine beam tracking algorithm for millimeter wave MISO systems," in *2018 IEEE International Conference on Communications Workshops (ICC Workshops)*, May 2018, pp. 1–6.

[16] M. Gao, B. Ai, Y. Niu, Z. Zhong, Y. Liu, G. Ma, Z. Zhang, and D. Li, "Dynamic mmWave beam tracking for high speed railway communications," in *2018 IEEE Wireless Communications and Networking Conference Workshops (WCNCW)*, April 2018, pp. 278–283.

[17] L. S. Pillutla and R. Annavajjala, "Integrated acquisition and tracking scheme for channel estimation in millimeter wave wireless networks," in *2017 IEEE 28th Annual International Symposium on Personal, Indoor, and Mobile Radio Communications (PIMRC)*, Oct 2017, pp. 1–5.

[18] E. Rastorgueva-Foi, M. Koivisto, M. Valkama, M. Costa, and K. Leppänen, "Localization and tracking in mmWave radio networks using beam-based DoD measurements," in *2018 8th International Conference on Localization and GNSS (ICL-GNSS)*, June 2018, pp. 1–6.

[19] C. Zhang, D. Guo, and P. Fan, "Tracking angles of departure and arrival in a mobile millimeter wave channel," in *2016 IEEE International Conference on Communications (ICC)*, May 2016, pp. 1–6.

[20] V. Va, H. Vikalo, and R. W. Heath, "Beam tracking for mobile millimeter wave communication systems," in *2016 IEEE Global Conference on Signal and Information Processing (GlobalSIP)*, Dec 2016, pp. 743–747.

[21] G. Li, Z. Wei, X. Zhang, and D. Yang, "Low overhead channel tracking strategy for millimetre wave multiple-input multiple-output system," *IET Communications*, vol. 11, no. 16, pp. 2544–2551, 2017.

[22] X. Gao, L. Dai, Y. Zhang, T. Xie, X. Dai, and Z. Wang, "Fast channel tracking for terahertz beamspace massive MIMO systems," *IEEE Trans. Veh. Technol.*, vol. 66, no. 7, pp. 5689–5696, July 2017.

[23] Y. Yapici and I. Güvenç, "Low-complexity adaptive beam and channel tracking for mobile mmwave communications," *arXiv e-prints*, arXiv:1811.11948, Nov. 2018.

[24] S. Shaham, M. Ding, M. Kokshoorn, Z. Lin, and X. Yao, "Fast channel estimation and beam tracking for millimeter wave vehicular communications," *arXiv e-prints*, arXiv:1806.00161, June 2018.

[25] L. Dai and X. Gao, "Priori-aided channel tracking for millimeter-wave beamspace massive MIMO systems," in *2016 URSI Asia-Pacific Radio Science Conference (URSI AP-RASC)*, Aug 2016, pp. 1493–1496.

[26] R. Van der Merwe, "Sigma-point Kalman filters for probabilistic inference in dynamic state-space models," Ph.D. dissertation, Oregon Health & Science University, 2004.

[27] S. Julier and J. Uhlmann, "Unscented filtering and nonlinear estimation," *Proc. IEEE*, vol. 92, no. 3, pp. 401–422, 2004.

[28] R. Horn and C. R. Johnson, "Topics in matrix analysis," 1991.

[29] D. H. Dini, D. P. Mandic, and S. J. Julier, "A widely linear complex unscented Kalman filter," *IEEE Signal Process. Lett.*, vol. 18, no. 11, pp. 623–626, Nov 2011.

[30] E. A. Wan and R. van der Merwe, "The unscented Kalman filter for nonlinear estimation," in *Proc. of IEEE Adaptive Syst. Signal Process. Commun. Control Symp. (ASSPCCS'00)*, 2000, pp. 153–158.

[31] H. M. T. Menegaz, J. Y. Ishihara, G. A. Borges, and A. N. Vargas, "A systematization of the unscented Kalman filter theory," *IEEE Trans. Autom. Control*, vol. 60, no. 10, pp. 2583–2598, Oct 2015.

[32] J. Choi, D. J. Love, and P. Bidigare, "Downlink training techniques for FDD massive MIMO systems: Open-loop and closed-loop training with memory," *IEEE J. Sel. Topics Signal Process.*, vol. 8, no. 5, pp. 802–814, Oct 2014.

[33] C. G. Baker, "Riemannian manifold trust-region methods with applications to eigenproblems," Ph.D. dissertation, Florida State University, 2008.

[34] C. F. Van Loan and N. Pitsianis, *Approximation with Kronecker Products*. Dordrecht: Springer Netherlands, 1993, pp. 293–314. [Online]. Available: https://doi.org/10.1007/978-94-015-8196-7_17

[35] S. Noh, M. D. Zoltowski, and D. J. Love, "Multi-resolution codebook and adaptive beamforming sequence design for millimeter wave beam alignment," *IEEE Trans. Wireless Commun.*, vol. 16, no. 9, pp. 5689–5701, Sept 2017.

[36] D. Ogbe, D. J. Love, and V. Raghavan, "Noisy beam alignment techniques for reciprocal MIMO channels," *IEEE Trans. Signal Process.*, vol. 65, no. 19, pp. 5092–5107, Oct 2017.

[37] A. J. Duly, T. Kim, D. J. Love, and J. V. Krogmeier, "Closed-loop beam alignment for massive MIMO channel estimation," *IEEE Commun. Lett.*, vol. 18, no. 8, pp. 1439–1442, Aug 2014.